Exploring LIGO sensitivity across binary black hole parameter space

LIGO SURF 2022 Second Interim Report
LIGO Technical Note T2200251

Daniela Hikari Yano[1],
Mentors: Richard Udall[2], Jacob Golomb[2] and Alan Weinstein[2]

[1]Barnard College
[2]California Institute of Technology, LIGO Laboratory

July 29th, 2022

Abstract

As we look ahead to LIGO, Virgo and KAGRA (LVK)'s next observational run (O4) and future gravitational wave observatories such as Cosmic Explorer, understanding the sensitivity of the detectors network for compact binary coalescences (CBCs) is important to estimating the merger rate density. The parameter space of CBCs is composed of fifteen parameters, which are used to characterize the binary systems. In this work, we explore how the network sensitivity (space-time sensitive hypervolume) changes according to changes in the CBC population parameter space. Using Monte Carlo simulations, we solve the averaged space-time sensitive hypervolume for different parameter configurations, marginalizing over subsets of the parameter space so that we can compare them.

1 Introduction

1.1 Overview of the study

Understanding the detector network sensitivity (space-time hypervolume VT) for GWs from CBCs is important for solving for the merger rate density, which is a key to understand the cosmic population and evolution of compact binaries. This works aims to study how the volume-time sensitivity of the LIGO, VIRGO and KAGRA network changes according to changes in the parameter space of coalescing binary systems. The parameter space of coalescing binary systems is composed of both intrinsic parameters (masses and spins) and extrinsic parameters (right ascension, declination, luminosity distance, inclination, polarization angle, time of coalescence, and phase at coalescence). This project will use available computational tools such as PyCBC[1] and Bilby [2] to generate waveforms produced from the merger of binary black holes (BBHs) and binary neutron stars (BNSs). By using Monte Carlo simulations, it will calculate the dependence of the space-time sensitive hypervolume on the selected parameters. The detections are defined using the predicted signal-to-noise ratio (SNR) of the injected signals, and is determined based on a SNR threshold. This study will be applied to estimate the space-time sensitive hypervolume of the next observation run

(O4) that is set to start running in March 2023, as well as to future GWs observatories.

1.2 Gravitational waves

In 2015, LIGO made its first direct detection of gravitational waves, GW150914 [3]. Since then GW signals from mergers of binary black holes and neutron stars have been detected. The third LIGO Scientific, Virgo and KAGRA (LVK) Collaboration Gravitational-Wave Transient Catalog (GWTC- 3) contains 90 GW signals from compact binary coalescences (CBCs) [4].
The space-time distortions caused by gravitational waves are transverse to direction of propagation. The LIGO detectors have two perpendicular 4km arms, each with a Michelson interferometer with a Fabry-Perot resonant cavity that allows to measure the change in the length of the arms [5]. This difference is used to calculate the strain, which is defined as $h = \Delta\mathrm{L}/\mathrm{L}$. The strain has a plus and a cross polarization:

$$h = h_+(t - z/c) + h_\times(t - z/c). \tag{1}$$

1.3 Signal-to-noise ratio (SNR)

This study uses simulations of waveforms over the parameter space. To quantify if a simulation of a strain would be detected this study uses the general noise-weighted inner product:

$$\langle a|b\rangle = 4\int_{f_{min}}^{f_{max}} \frac{a^*(f)b(f)}{S_n(f)}df \tag{2}$$

where S_n is the Power spectral density (PSD). The optimal SNR (ρ) is calculated using equation 2, where $\rho^2 = \langle h|h\rangle$. The SNR is calculated for each detector, and the estimated SNR of all the detectors in the network can be calculated as the square root of their individual SNRs squared:

$$\rho = \sqrt{\rho_{H1}^2 + \rho_{L1}^2 + \rho_{V1}^2} \tag{3}$$

where ρ_{H1} stands for the SNR of the Hanford observatory, ρ_{L1} the SNR of the Livingston observatory, and ρ_{V1} the SNR of Virgo. If the SNR is above a threshold, it could be detected.

1.4 Space-time sensitive hypervolume

Estimating the merger rate density is important to understanding the cosmic population. The mean number of signals of astrophysical origin Λ_1 above the chosen threshold, is related to R, the rate density (events per unit time per comoving volume) of binary coalescenses, by [6]:

$$\Lambda_1 = R\langle VT\rangle \tag{4}$$

where $\langle VT\rangle$ is the averaged space-time sensitive hypervolume, which is the main topic of this study and is described by the following equation:

$$\langle VT\rangle = T\int d\Omega \int \eta(z,\vec{\lambda})C(z)D_L^2(z)dz \tag{5}$$

where $\eta(\vec{D_L},\lambda)$ is the efficiency function, and D_L is the luminosity distance. In equation 5, $C(D_L)$ incorporates all cosmological effects:

$$C(z) = \frac{c}{H_0}\frac{1}{(1+z)^3E(z)} \tag{6}$$

2 Methodology

It is not possible to calculate the space-time sensitive hypervolume (Eq. 5) analytically. The Monte Carlo integration is used to compute an estimate of its integral using random sampling. Therefore, it is necessary to generate populations of CBCs waveforms to numerically solve for the space-time sensitive hypervolume.

2.1 Generating waveforms

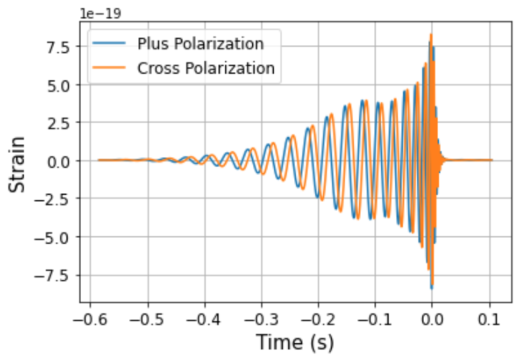

Figure 1. An example of a simulated waveform in time domain. The waveform was generated for black holes of 35 $M_{\odot}$, at a distance of 1 Mpc, using the IMRPhenomXP approximant. The waveform is tapered to zero at frequencies below 20 Hz because of computational costs.

This project uses PyCBC [1], a software package, that has methods that generate waveforms in the time and frequency domains. The methods to generate those waveforms received as input an approximant waveform model families, such as IMRPhenomXP [7, 8][] and the following parameters: masses, spins, inclination, phase at coalescence, and luminosity distance. It returns the cross and plus polarization of the waveform. It is necessary to take into account the detector antenna response to each polarization, as in [9]:

$$h = h_{+}F_{+} + h_{\times}F_{\times} \tag{7}$$

where F_{+} and $F_{\times}$ depend on right ascension, declination, and polarization angle.

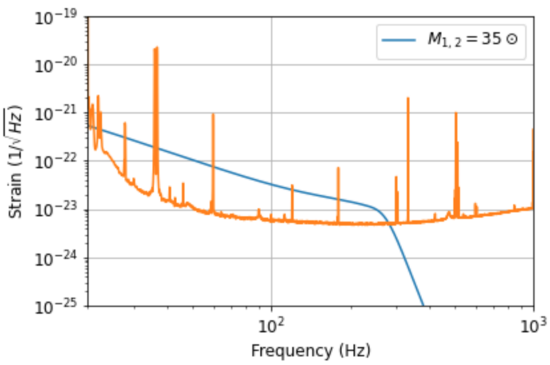

Figure 2. An example of a simulated waveform in frequency domain. The blue line is the waveform simulated for a black hole merger of masses 35 $M_{\odot}$, at a distance of 1 Mpc. The orange line is the noise of the detector for O3 in the Hanford detector.

2.2 Generating populations

In this project, the generation of the CBCs population is carried in three steps. In each of those steps, the parameters are generated according to probability distributions. The first step is drawing the parameters necessary to generate the CBCs waveforms: masses, spins components, inclination, and phase at coalescence. For each of those configurations, the waveform are generated at a luminosity distance of 1 Mpc.

The second step is drawing the sky parameters (right ascension, declination, and polarization) from the prior probability distribution. The sky parameters are used to calculate the detector antenna response as shown in Eq. 7. For each waveform generated in the first step, N number of sky configurations are draw, and the corresponding SNR is calculated.

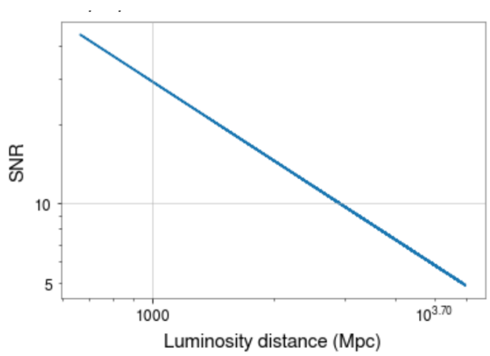

Figure 3. SNR for 100 samples for different luminosity distances, in logarithm scale. All the other parameters were kept fixed. Mass 1 is 35 $M_{\odot}$, mass 2 is 35 $M_{\odot}$, and all the other parameters were set to zero.

The last step is scaling the SNR according to an established number of luminosity distances. That is possible because, as shown in Figure 3, there is a relationship between the SNR and the luminosity distance (SNR$\propto 1/D_L$). Therefore, a number of luminosity distances are draw from probability distributions for each of the SNRs calculated in the second step. Then, they are scaled accordingly. The scaling of the SNR using the luminosity distance is a desired operation because it is computationally faster than generating a new waveform for each distance. However, it is important to note that the masses are generated drawing from $p(\vec{\theta_{det}})$, and mass is degenerate with redshift:

$$m_{det} = (1 + z)m_{source} \tag{8}$$

Therefore, it is necessary to account for this in the calculation, especially because if we just correct the masses to the correct frame, then the masses of population is not going to follow the mass probability density.

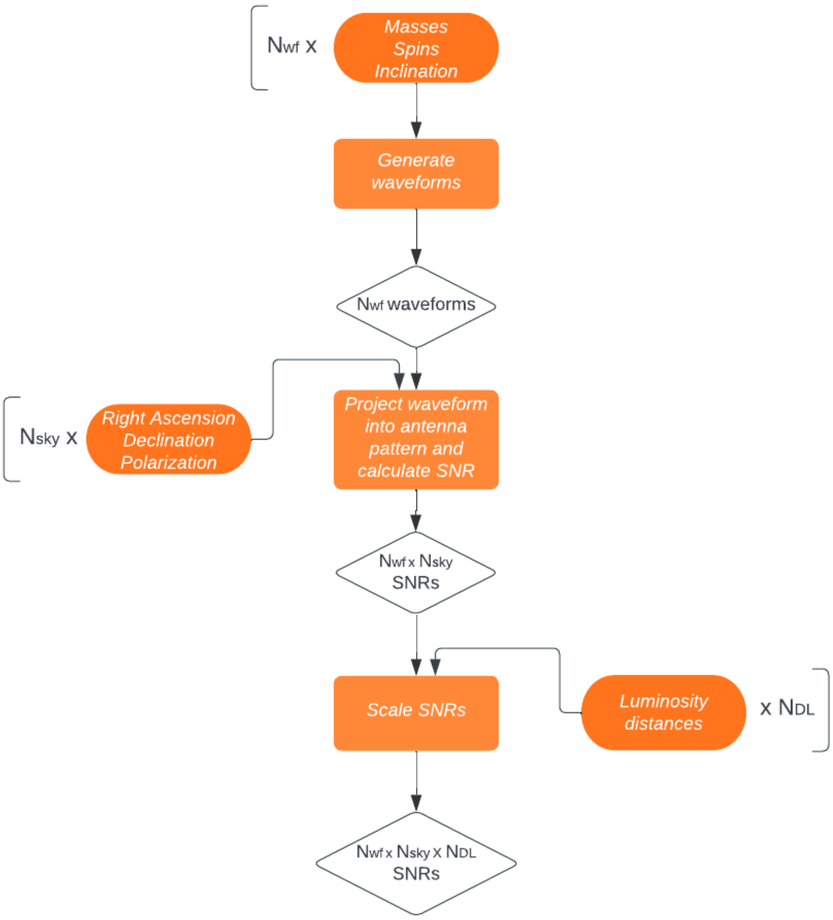

Figure 4. Flowchart showing the pipeline used by SIFCE [10] to generate a population and calculate SNRs.

2.3 Space-time sensitive hypervolume estimation

Using Monte Carlo, Eq. 5 can be estimated as a sum:

$$\langle VT \rangle = \frac{1}{|\Gamma|} \sum_{\vec{\theta} \in \Gamma} \omega(z) p_{det}(\vec{\theta}) \tag{9}$$

where:

$$\omega(z) = C(z) D_L^2(z). \tag{10}$$

3 Experiments

3.1 Calculating the variance of the space-time sensitive hypervolume

As we are using Monte Carlo to numerically solve for the space-time sensitive hypervolume, it is important to understand how precise the estimations are and how it varies with the size of the population. In this experiment, our population is composed of BNSs and we are studying the variance of the estimated space-time sensitive hypervolume estimation. We chose to use a BNS population because the detection of BNSs mergers are constrained to smaller redshifts, so the effects of the mass degeneracy are almost negligible. In this study, the maximum luminosity distance is 400 Mpc, for which the redshift using Planck18 cosmology [11] is ~ 0.0849.

Therefore, we are not carrying corrections for the masses frames. Here, m_1 is draw from Gaussian distributions with mean of 1.5 $M_\odot$ and standard deviation of 0.05 $M_\odot$:

$$p(m_1) \propto \frac{1}{0.05\sqrt{2\pi}} e^{-\frac{1}{2}\frac{(m_1-1.5)}{0.05}} \quad (11)$$

and the mass ratio has a probability distribution following a power law:

$$p(m_{ratio}) \propto m_{ratio}^2 \quad (12)$$

and is has a minimum of 0.9 and a maximum of 1. The spins components of the binary stars are set to zero.

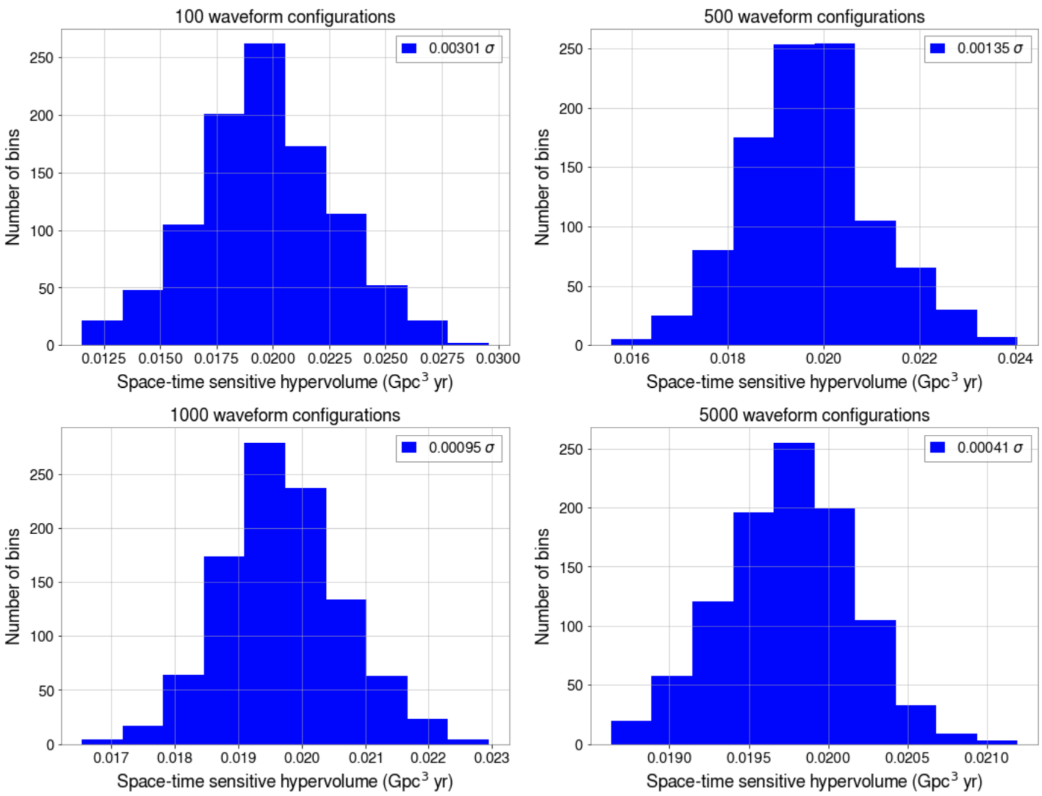

Figure 5. The space-time sensitive hypervolume distribution, when computer over different number of waveform configurations.

4 Progress and next steps

During the last weeks, I contributed to the development of Simple Injection Framework for Computational Estimates (SIFCE), a software package that performs the procedure described in the Methodology. More specifically, I worked on the implementation of the methods to compute the space-time sensitive hypervolume, and in the methods to generate and organize the data frame that stores the parameters of the CBCs. The next step is to conduct experiments with the SIFCE to study the dependence of the space-time sensitive hypervolume distribution in the parameter space.

5 Acknowledgements

I thank Alan Weinstein, Richard Udall, and Jacob Golomb for their tremendous support in this project. I also gratefully acknowledge the support from the National Science Foundation Research Experience for Undergraduates (NSF REU) program, the California Institute of Technology, and the LIGO Summer Undergraduate Research Fellowship.

References

[1] Alex Nitz, Ian Harry, Duncan Brown, Christopher M. Biwer, Josh Willis, Tito Dal Canton, Collin Capano, Thomas Dent, Larne Pekowsky, Andrew R. Williamson, Gareth S Cabourn Davies, Soumi De, Miriam Cabero, Bernd Machenschalk, Prayush Kumar, Duncan Macleod, Steven Reyes, dfinstad, Francesco Pannarale, Thomas Massinger, Sumit Kumar, Márton Tápai, Leo Singer, Sebastian Khan, Stephen Fairhurst, Alex Nielsen, Shashwat Singh, Koustav Chandra, shasvath, Bhooshan Uday, Varsha Gadre. *gwastro/pycbc*. DOI: `10.5281/zenodo.5347736`.

[2] Gregory Ashton et al. "BILBY: A user-friendly Bayesian inference library for gravitational-wave astronomy". In: *The Astrophysical Journal Supplement Series* 241.2 (2019), p. 27.

[3] Benjamin P Abbott et al. "Observation of gravitational waves from a binary black hole merger". In: *Physical review letters* 116.6 (2016), p. 061102. DOI: `https://doi.org/10.1103/PhysRevLett.116.061102`.

[4] R Abbott et al. "GWTC-3: compact binary coalescences observed by LIGO and Virgo during the second part of the third observing run". In: *arXiv preprint arXiv:2111.03606* (2021). DOI: `https://doi.org/10.48550/arXiv.2111.03606`.

[5] Junaid Aasi et al. "Advanced ligo". In: *Classical and quantum gravity* 32.7 (2015), p. 074001. DOI: `https://doi.org/10.48550/arXiv.1411.4547`.

[6] Benjamin P Abbott et al. "The rate of binary black hole mergers inferred from Advanced LIGO observations surrounding GW150914". In: *The Astrophysical journal letters* 833.1 (2016), p. L1. DOI: `https://doi.org/10.48550/arXiv.1602.03842`.

[7] Geraint Pratten et al. "Computationally efficient models for the dominant and subdominant harmonic modes of precessing binary black holes". In: *Physical Review D* 103.10 (2021), p. 104056.

[8] Geraint Pratten et al. "Setting the cornerstone for a family of models for gravitational waves from compact binaries: The dominant harmonic for nonprecessing quasicircular black holes". In: *Physical Review D* 102.6 (Sept. 2020). DOI: `10.1103/physrevd.102.064001`. URL: `https://doi.org/10.1103%2Fphysrevd.102.064001`.

[9] John Whelan. "Visualization of antenna pattern factors via projected detector tensors". In: *LIGO Document T1100431-v2* 6 (2012).

[10] Richard Udall, Jacob Golomb, and Daniela Yano. *Simple Injection Framework for Computational Estimates (SIFCE)*. `https://git.ligo.org/richard.udall/sifce`. 2022.

[11] Planck Collaboration et al. "Planck 2018 results. VI. Cosmological parameters". In: (2020).